Journal of Thermal Analysis and Calorimetry, Vol. 79 (2005) 451–454

INFLUENCE OF pH ON IRON DOPED Zn_2TiO_4 PIGMENTS

S. C. Souza[1], *I. M. G. Santos*[1*], *M. R. S. Silva*[1], *M. R. Cássia-Santos*[1], *L. E. B. Soledade*[1], *A. G. Souza*[1], *S. J. G. Lima*[2] *and E. Longo*[3]

[1]LTM, Departamento de Química/CCEN, Universidade Federal da Paraíba, Campus I, CEP 58059-900, João Pessoa, PB, Brazil
[2]Laboratório de Solidificação Rápida / CT, UFPB, João Pessoa, PB, Brazil
[3]LIEC, Departamento de Química, Universidade Federal de São Carlos, São Carlos, SP, Brazil

Zinc titanate, Zn_2TiO_4, can be used as ceramic pigment, due to its stability up to approximately 1550°C and chemical inertia. This work aims to obtain ceramic pigments, using the polymeric precursor method, based on zinc titanate spinel (Zn_2TiO_4), containing 5 mol% of iron. The synthesis was carried out with pH values of 1, 7 and 10, in order to verify the influence of the chelation upon the obtained color. The characterization of the samples was performed by termogravimetric analyses, X-ray diffraction and colorimetry. The crystallite size decreases with the increase of pH. The segregation of zinc oxide or titanium oxide was observed, according to the pH of the polymeric resin. The pH of the synthesis changed the color of pigment due to the iron ligand field.

Keywords: *inverse spinel, iron, pH*

Introduction

Ceramic pigments are predominantly inorganic compounds, being insoluble and inert in glazes and ceramic pastes. The quality of a ceramic pigment depends on its optical and physical properties. These properties are directly related to the crystalline structure of the pigment, its chemical composition, purity, stability, and some physical characteristics, such as particle size distribution, particle shape, surface area, etc. [1]. Color is an important feature of many ceramic products [2].

According to Eppler [3, 4], titanium oxide can be combined with zinc oxide, yielding a white color spinel. The objective of this work is to obtain ceramic pigments, using the polymeric precursor method [5–8], based on zinc titanate spinels (Zn_2TiO_4), doped with iron. The synthesis was done with three different pH values, in order to verify the influence of chelation on the obtained color.

Zn_2TiO_4 displays an $A[AB]O_4$ type inverse spinel structures. It presents the possibility of formation of substitutional solid solution with transition metals, thus enlarging the number of colors that can be obtained.

A great advantage of the polymeric precursor method, in relation to other chemical synthesis methods, is its low cost, once the reagents used in larger amounts are relatively cheap, besides working at relatively low temperatures.

Experimental

The first step is the synthesis of titanium citrate, in which 3:1 citric acid:metal molar ratio was used, to guarantee a limpid and transparent solution. In a beaker under intense stirring and agitation citric acid was dissolved in distilled water and heated to approximately 70°C. After the complete dissolution of citric acid, titanium isopropoxide was slowly added, thus forming a white precipitate that was dissolved upon stirring before a new isopropoxide addition. After addition of all isopropoxide, the substance was left in the beaker and stirred while a limpid and transparent titanium citrate solution was obtained.

Zinc nitrate and citric acid were added to the titanium citrate solution to maintain 3:1 citric acid:metal molar ratio. Then, ammonium hydroxide was added to adjust pH. Finally, ethylene glycol was added to the solution, to achieve 40:60% ethylene glycol:citric acid ratio in order to promote the esterification and the formation of the polymeric resin. After addition of all the reagents, the solution was heated up approximately to 110°C to form a polymeric gel.

Then, the samples were calcined at 350°C for 30 min, leading to the formation of the powder precursors. These precursors were de-agglomerated and ground, and passing through a 120 mesh sieve. These powder precursors were submitted to a second heat treatment at 500, 600, 700, 800, 900 and 1000°C for 1 h in an oven.

The powder precursors were analyzed by thermal analysis. TG/DTG curves were obtained in a TGA-50

* Author for correspondence: ieda@dalton.quimica.ufpb.br

1388–6150/$20.00

Akadémiai Kiadó, Budapest, Hungary
Springer, Dordrecht, The Netherlands

Shimadzu thermobalance, and the DTA curves were recorded using a Shimadzu DTA-50 analyzer. Air atmosphere was used, with a flow rate of 100 mL min^{-1} and the heating rate was of 15 K min^{-1}. Small alumina crucibles and about 5 mg initial sample masses were used. Both thermal analyses were carried out between room temperature and 950°C.

The X-ray diffraction patterns were determined in a Siemens D-5000 diffractometer using a monochromatic iron K_α target.

The L*, a* and b* color parameters of samples were measured through the Gretac Macbeth Color-eye spectrophotometer 2180/2180 UV, in the 360–750 nm range, using the D65 illumination. The CIE-L *a *b * colorimetric method, recommended by the CIE (Commission Internationale de l'Eclairage) was followed. In this method, L* is the lightness axis [black (0) white (100)], b* is the blue (–) yellow (+) axis and a* is the green (–) red (+) axis.

Results and discussion

The results of the TG/DTG analyses are presented in Figs 1 and 2. Two main decomposition steps were recorded for all studied spinels. The first one is related to the loss of water and the evolution of some adsorbed gases on the surface of the powder precursors. The second event was attributed to the decomposition of the organic matter and to the oxidation of metal cations [9]. All the other TG/DTG curves presented the same profile observed in Fig. 2. The thermoanalytical results are summarized in Tables 1 and 2.

Table 1 Temperature and mass loss values determined by TG

Spinel	Event	T_{range}/°C	Mass loss/%
Zn_2TiO_4	1	43–91	5
	2	352–560	59
5% Fe/pH=1	1	39–101	7
	2	321–542	49
5% Fe/pH=7	1	39–97	10
	2	348–677	79
5% Fe/pH=10	1	46–137	11
	2	327–578	80

Table 2 DTG and DTA peak temperatures of pure Zn_2TiO_4 and iron doped spinals at different pH values

Spinel	DTG peak temperature/°C	DTA peak temperature/°C
Zn_2TiO_4	474	476
5% Fe/pH=1	466	459
5% Fe/pH=7	560	543
5% Fe/pH=10	529	532

Two different behaviors were observed. One for the powder precursor of undoped zinc titanate and the iron doped zinc titanate synthesized at pH=1. These samples exhibited lower peak temperatures and lower

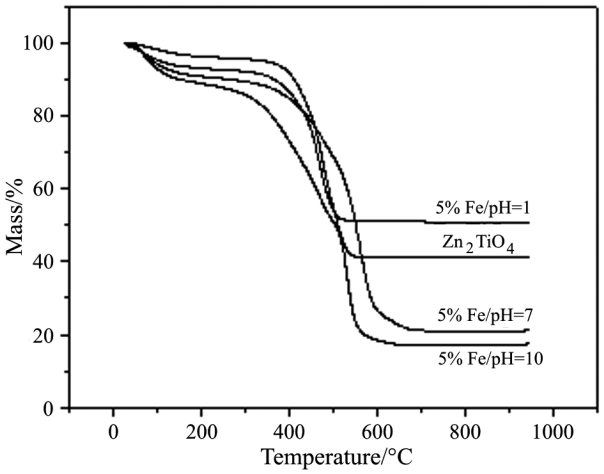

Fig. 1 TG curves of the Zn_2TiO_4 spinel powder precursors at pH=1, and of $Zn_{1.90}Fe_{0.10}TiO_4$ at pH=1, 7 and 10

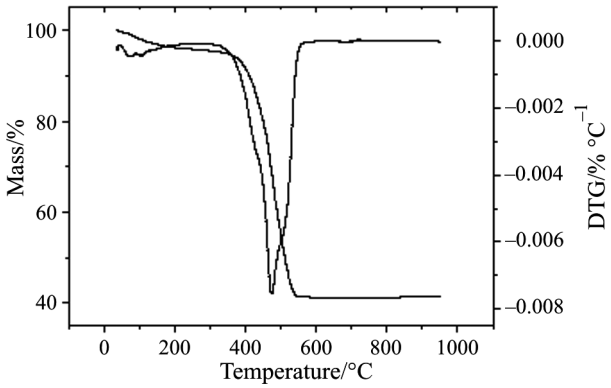

Fig. 2 TG/DTG curves of Zn_2TiO_4 spinel powder precursor

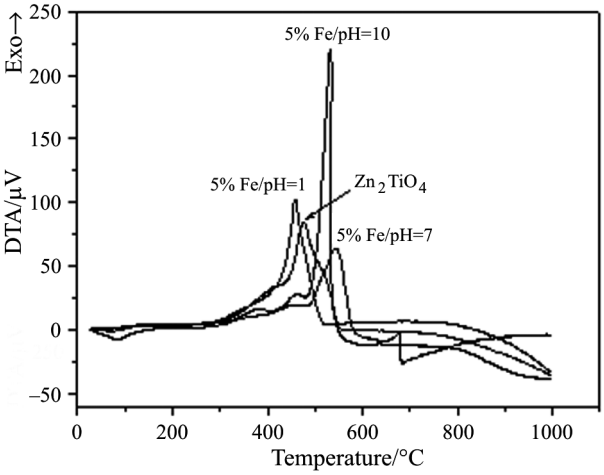

Fig. 3 DTA curves of Zn_2TiO_4 spinel powder precursors at pH=1, and of $Zn_{1.90}Fe_{0.10}TiO_4$ at pH=1, 7 and 10

mass losses. An opposite behavior was shown for the precursors of iron doped zinc titanate samples synthesized at higher pH values (pH=7 and 10).

From these results it was verified as the pH increases 1–10, the obtained mass losses raise from 49 to 80%. It was also observed that the decomposition temperature increases when the pH raises from 1 for 7, but at pH=10 it was decreased. These differences are due to polymerization, since an increased pH of the solution enhances the dissociation of protons from carboxylic acid in citric acid, making more complicated the ester reactions [7].

The DTG peak temperatures (Table 2) for the spinels Zn_2TiO_4 and $Zn_{1.90}Fe_{0.10}TiO_4$ synthesized at pH=1, 7 and 10, were: 474, 466, 560 and 529°C, respectively.

The DTA curves are collected in Fig. 3. The exotherm peaks are related to the combustion of the organic matter. These peak temperatures are presented in the Table 2, together with the DTG peak temperatures. A good agreement was observed between these peak temperatures.

The X-ray patterns show the phase formation as a function of the calcination temperature for undoped Zn_2TiO_4 (Fig. 4). The diffraction peaks are characteristic to the Zn_2TiO_4 phase which appeared at 500°C. The raising temperature promotes the increase of the crystallinity of this system, evidenced by the narrower bands and enchanced intensities of the diffraction peaks ascribed to the Zn_2TiO_4 phase. The XRD patterns indicate a single phase system, once no secondary or intermediate phases were detected.

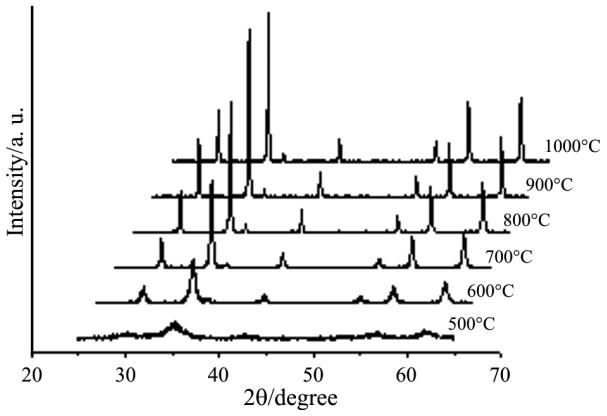

Fig. 4 X-ray diffraction patterns of Zn_2TiO_4 spinel after calcination between 500 and1000°C

Figure 5 summarizes the XRD patterns of Zn_2TiO_4 spinels before and after the partial replacement of zinc by 5 mol% of iron, at pH=1, 7 and 10, heat treated at 1000°C. It can be verified that undoped Zn_2TiO_4 is a single phase system, within the detection limit of the X-ray apparatus, whilst $Zn_{1.90}Fe_{0.10}TiO_4$ displays a secondary phase. At pH=1 and 7, the secondary phase was zinc oxide, ZnO, however, at pH=10 it was identified as a precipitated of titanium oxide (TiO_2).

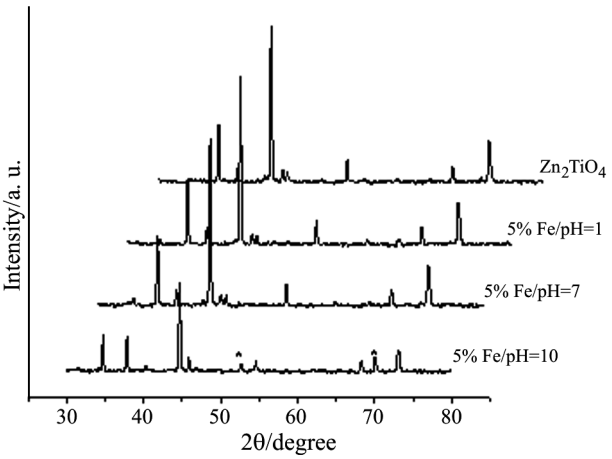

Fig. 5 XRD patterns of the Zn_2TiO_4 spinel before and after a partial replacement of zinc by 5 mol% of iron at pH=1, 7 and 10. For the undoped Zn_2TiO_4, synthesis was done at pH=1

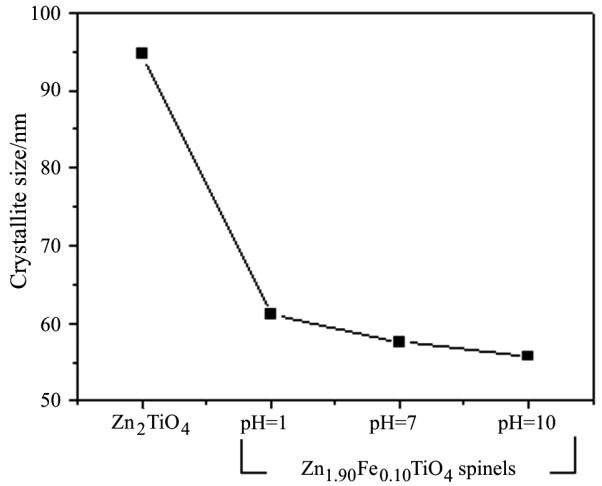

Fig. 6 Evolution of the crystallite size of Zn_2TiO_4 and of $Zn_{1.90}Fe_{0.10}TiO_4$

From the Scherrer equation [10] (Eq. (1)) and using the data taken from Figs 4 and 5, the crystallite sizes were calculated, as presented in Fig. 6.

$$t = \frac{0.9\lambda}{\beta \cos\theta} \quad (1)$$

where λ is the $FeK_{\alpha 1}$ wavelength, θ is the diffraction angle, β is the full width at half maximum (FWHM) of the diffraction peak, calculated by the equation $\beta = (B_{obs}^2 - b^2)^{1/2}$, in which B_{obs} is the FWHM obtained for the sample and b the FWHM of a standard, quartz.

In this figure, a reduction in the crystallite size with increasing pH of solutions was observed. That

Table 3 Chromatic coordinates of the pigments after calcination at 1000°C

	L*	a*	b*
Zn_2TiO_4	91.886	1.432	4.440
$Zn_{1.9}Fe_{0.1}TiO_4$ – pH=1	83.950	10.751	34.978
$Zn_{1.9}Fe_{0.1}TiO_4$ – pH=7	85.947	8.866	28.132
$Zn_{1.9}Fe_{0.1}TiO_4$ – pH=10	84.998	9.016	29.326

decrease is a consequence of the precipitation of TiO_2 or ZnO, leading to a distortion in the Zn_2TiO_4 lattice.

Chromatic coordinates are presented in Table 3. All samples became darker, when iron was added to the pigment, with more pronounced yellow and red colors. This result is more important for samples synthesized at pH=1, specially for b* coordinate. Since the secondary phases are colorless (ZnO and TiO_2), the observed differences are probably due to the iron ligand field and oxidation state. According to the literature, the octahedral field presents a higher energy than the tetrahedral one. This is due to the presence of six oxygen ligands instead of four [11]. Another important point is the electron configuration of Fe^{3+} and Fe^{2+}. Fe^{3+} presents a d^5 configuration and weak ligands leading to a high spin state, with forbidden d–d transitions, which are very weak. On the other hand, Fe^{2+} has a d^6 configuration, with a pair spin, leading to strong colors due to the d–d electronic transitions [12].

Conclusions

Undoped zinc titanate, Zn_2TiO_4, and iron substituted samples (up to 5 mol% of iron) were successfully synthesized by the polymeric precursor method, at pH=1, 7 and 10. The powder precursors were studied using TG/DTG and DTA methods, and two decomposition steps were recorded. The first one was attributed to the elimination of water and of some adsorbed gas molecules. The second stage was ascribed to the thermal decomposition of organic groups (such as carboxyls and carbonyls) and carbonates. From the X-ray diffraction results it was verified that the undoped Zn_2TiO_4 spinels are single phase compounds. For the pigments in which the zinc was substituted by 5 mol% of iron, at pH=1 and 7, the formation of ZnO secondary phase occurred and at pH=10, the precipitation of TiO_2 was favored. Upon the increase of the pH of the polymeric resin, the crystallite size decreased due to the segregation of zinc oxide or titanium oxide. Samples synthesized at pH 1 presented higher a* and b* values, indicating that the change in the pH of the solution also changes iron ligand field and/or the oxidation state.

Acknowledgements

The authors acknowledge the Brazilian agency CNPq and Banco do Nordeste do Brasil (BNB) for their financial support of this work.

References

1 F. Bondioli, T. Manfredini and A. P. N. Oliveira, Ceramica Industrial, 3 (1998) 13.
2 A. Burgyan and R. A. Eppler, Ceram. Bull., 12 (1982) 1001.
3 R. A. Eppler, Am. Ceram. Soc. Bull., 60 (1981) 562.
4 R. A. Eppler, J. Am. Ceram. Soc., 66 (1983) 794.
5 N. Pechini, U.S. Patent number 3.330.697, July 1967.
6 P. A. Lessing, Ceram. Bull., 68 (1989) 1002.
7 M. Kakihana and M. Yoshimura, Bull. Chem. Soc. Jpn., 72 (1999) 1427.
8 E. R. Leite, C. M. G. Souza, E. Longo and J. A. Varela, Ceram. Int., 21 (1995) 143.
9 C. S. Xavier, C. E. F. Costa, S. C. L. Crispim, M. I. B. Bernardi, M. A. M. A. Maurera, M. M. Conceição, E. Longo and A. G. Souza, J. Therm. Anal. Cal., 75 (2004) 461.
10 B. D. Cullity, Elements of X-ray Diffraction – Addison-Wesley Publishing Company, Inc., Massachusetts, USA 1956.
11 K. Nassau, The Physics and Chemistry of Color – the Fifteen Causes of Color – John Wiley & Sons, New York, USA 1983.
12 J. E. Huheey, Inorganic Chemistry – Principles of Structure and Reactivity – Harper & Row, London, United Kingdom 1975.